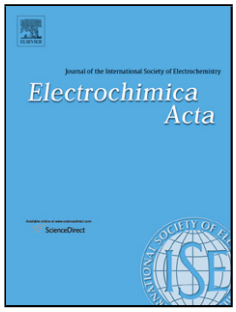

Title: Redox behaviour of G-quadruplexes

Author: Ana-Maria Chiorcea-Paquim Ana Maria Oliveira-Brett

PII: S0013-4686(13)01419-9
DOI: http://dx.doi.org/doi:10.1016/j.electacta.2013.07.150
Reference: EA 20943

To appear in: *Electrochimica Acta*

Received date: 4-6-2013
Revised date: 17-7-2013
Accepted date: 18-7-2013

Please cite this article as: A.-M. Chiorcea-Paquim, A.M. Oliveira-Brett, Redox behaviour of G-quadruplexes, *Electrochimica Acta* (2013), http://dx.doi.org/10.1016/j.electacta.2013.07.150

Redox behaviour of G-quadruplexes

Ana-Maria Chiorcea-Paquim and Ana Maria Oliveira-Brett*

Departamento de Química, Faculdade de Ciências e Tecnologia, Universidade de Coimbra,

3004-535 Coimbra, Portugal

* To whom correspondence should be addressed
Ana Maria Oliveira-Brett
Departamento de Química,
Faculdade de Ciências e Tecnologia,
Universidade de Coimbra,
3004-535 Coimbra, Portugal
Phone: 00351239854487
e-mail: brett@ci.uc.pt

Abstract

Guanine rich nucleic acids can self-assemble into four-stranded guanine (G)-quadruplex structures that have been identified in eukaryotic telomeres, as well as in non-telomeric genomic regions, such as gene promoters, recombination sites and DNA tandem repeats, finding wide applications in areas ranging from medical chemistry to nanotechnology and biosensor technology. In addition to classical methodologies for studying G-quadruplex structures, such as circular dichroism, nuclear magnetic resonance or crystallography, the electrochemical methods present very high sensitivity and selectivity and have been used for the rapid detection of the conformational changes from single-strand to G-quadruplex. This review is focused on the recent advances of G-quadruplexes electrochemistry and the design of strategies for the fabrication of G-quadruplex-based biosensors with electrochemical detection, in particular G-quadruplex aptasensors and hemin/G-quadruplex peroxidase-mimicking DNAzymes biosensors.

*Keywords***:** G-quadruplex, G-quartet, aptasensor, DNAzyme, DNA electrochemical biosensor.

Table of contents

1 Overview

Guanine (G) rich nucleic acid sequences present the ability to self-assemble into four-stranded helical arrangements called G-quadruplexes (**Scheme 1**), that are found in telomeric regions of chromosomes, oncogene promoter sequences and other biologically relevant regions of the genome [1-13]. The building blocks of G-quadruplexes are structures known as G-quartets (G_q) (**Scheme 1B**), which correspond to the association of four planar G bases held together by eight Hoogsteen hydrogen bonds. The G-quartets are stack on top of each other in a helical fashion and are stabilized by π-π hydrophobic interactions and by the presence of monovalent cations such as K^+ and Na^+. The cations are placed in the central helical cavity, in between the G-quadruplex plain, and establish interactions with the carbonyl oxygen from the G bases.

G-quadruplexes are very polymorphic, being classified in terms of their molecularity (i.e. the number of associated strands, leading to the formation of monomer, dimer or tetramer quadruplexes, **Scheme 1C**), strand polarity (i.e. the relative arrangement of adjacent strands in parallel or antiparallel orientations), glycosidic torsion angle (anti or syn) and orientation of the connecting loops (lateral, diagonal or both) [1, 4, 13-15]. Different quadruplex topologies have been observed by nuclear magnetic resonance (NMR) or crystallography, either as native structures or as complexes with small-molecules.

G-quadruplex structures are relevant in areas ranging from structural biology to medical chemistry, supra-molecular chemistry, nanotechnology and biosensor technology. They have emerged as a new class of cancer-specific molecular targets for anticancer drugs, since the quadruplex stabilisation by small organic molecules can lead to telomerase

inhibition and telomere dysfunction in cancer cells [8, 9, 13]. In addition, G-rich oligonucleotides are able to self-organize in quadruplex-based two-dimensional networks and long nanowires, relevant for nanotechnology applications [16-21].

Different review articles summarized the recent literature on the structure and stability of G-quadruplexes that are relevant for *in vivo* function and drug design [1, 4, 5, 22], and assembly of G-quadruplex nanostructures and devices [23]. G-quadruplex structures were studied using different experimental techniques, such as molecular absorption, circular dichroism, molecular fluorescence, mass spectrometry, NMR, surface plasmon resonance, crystallography or atomic force microscopy (AFM) [24-27].

Electrochemical techniques present very high sensitivity and selectivity and can be successfully employed for the rapid detection of small perturbations in the nucleic acid secondary structure, and recently started to be used for the detection of G-quadruplex configurations [28]. Electrochemical sensing devices based on quadruplex nucleic acids have the advantage of being highly selective and sensitive, fast, accurate, compact, portable, and inexpensive. For the first time the recent advances on G-quadruplex electrochemistry and G-quadruplex-based electrochemical biosensors are reviewed.

2 G-quadruplex electrochemistry

Although electrochemical research on DNA is of great relevance to explain many biological mechanisms and the nucleic acids redox behaviour and adsorption processes have been extensively studied over recent decades [29-35], the redox behaviour of G-quadruplex structures stared to be investigated only very recently [28].

The first report on the electrochemical oxidation of G-quadruplex structures used differential pulse (DP) voltammetry at a glassy carbon (GC) electrode [36]. The voltammetric behaviour of two sequences: thrombin-binding aptamer, TBA (5'-GGTTGGTGTGGTTGG-3') and extended thrombin-binding aptamer, eTBA (5'-GGGTTGGGTGTGGGTTGGG-3'), (**Scheme 2**), was correlated with the sequence base composition, the presence/absence of K^+ ions, and the adsorption morphology on a highly oriented pyrolytic graphite (HOPG) surface was investigated by AFM.

DP voltammograms obtained in Na^+ ions solutions of TBA (**Fig. 1A**) and eTBA (**Fig. 1D**) showed only the occurrence of the oxidation of guanine (G) residues at the C_8-H position, in a two-step mechanism involving the total loss of four electrons and four protons, anodic peak G [28, 36, 37]. AFM images of TBA (**Fig. 1B)** and eTBA (**Fig. 1E**) showed two different morphologies, a thin network film due to the adsorption of the single-stranded molecules and spherical and rod-like shapes aggregates due to the adsorption of some G-quadruplex structures.

DP voltammograms obtained in K^+ ions containing solutions showed a decrease of the guanine oxidation peak G, and, in the case of eTBA, the occurrence of a new peak at higher potential, due to the oxidation of G-quartets (G_q) (**Figs. 1A and 1D**). The oxidation peak G_q did not appeared in the experiments with TBA, due to the very little concentration of G-quartets, below DP voltammetric detection limit. The voltammetric results were confirmed by the AFM images, showing that in the presence of K^+, TBA (**Fig. 1C**) and eTBA (**Fig. 1F**) adsorbed less onto HOPG, when compared to the adsorption in the presence of only Na^+ ions, and the morphology corresponded only to the adsorption of single-stranded molecules. This is due to the fact that, in the presence of K^+, TBA and eTBA form monomeric intra-molecular quadruplexes arranged in a chair-like structure and

consisting of two G-quartets connected by two TT loops and a single TGT loop (**Scheme 2**) [38], that are very stable, compact and rigid, preventing the interaction with the hydrophobic HOPG surface [36].

The interaction between TBA and eTBA sequences with the serine protease thrombin was studied using voltammetry and AFM, and the mechanism of interaction was established [28, 39]. The AFM results obtained after the incubation of thrombin with single-stranded aptamers (**Figs. 2A and 2D**) showed for low incubation times the co-adsorption of molecules of the aptamer–thrombin, the free aptamer and the free thrombin. Increasing the incubation time, the height of the aggregates increased in agreement with the formation of an aptamer-thrombin complex. The voltammetric results confirmed these data and showed that thrombin oxidation peaks T1 and T2 occur at a more positive potential upon the aptamer-thrombin complex formation (**Figs. 2C and 2F**). This behaviour was explained considering coiling of the single-stranded aptamers around the thrombin structure, leading to the formation of a robust complex that maintains the conformation of the thrombin molecules.

After incubation of thrombin with G-quadruplex aptamers (**Figs. 2B and 2E**), the AFM images showed patches of a thick layer with a bulky, knotty appearance due to the existence of a large number of embedded aggregates, corresponding to the adsorption of different types of aggregates dictated by the interaction with either one or both thrombin exocites. The voltammetric data (**Figs. 2C and 2F**) suggested that upon interaction with thrombin, the quadruplexes are always in contact with the electrode surface whereas the thrombin molecules lie above the quadruplex structure which reduces their contact with the electrode surface leading to the occurrence of lower thrombin oxidation peaks.

The redox behaviour and the adsorption mechanism of 10-mer oligonucleotides that contain only one block of guanines, $d(G)_{10}$, $d(TG_9)$ and $d(TG_8T)$, with respect to their ability to form parallel tetra-molecular G-quadruplexes was described [28, 40, 41]. The voltammetric and AFM experiments showed the oxidation of $d(G)_{10}$, $d(TG_9)$ and $d(TG_8T)$ at the GC electrode, and spontaneous adsorption onto HOPG surface (**Figs. 3 and 4**), with the formation and stabilization of G-quadruplexes and different higher-order nanostructures, directly influenced by the oligonucleotides base composition [40], concentration [41] and pH of the solution [41].

Single-stranded sequences were obtained in Na^+ containing solutions for short incubation times and were detected in AFM as thin polymeric structures (**Fig. 3B**) and in DP voltammetry by the occurrence of only the oxidation peak G (**Fig. 3A**). G-quadruplex secondary structures were formed very slowly in Na^+ ions containing solutions (**Figs. 3A and 3C**), and very fast in freshly prepared K^+ ions containing solutions, by AFM the adsorption of higher spherical aggregates was imaged, and by DP voltammetry the decrease of oxidation peak G and the occurrence/increase of oxidation peak G_q, and a shift to positive potentials, in a K^+ ions concentration and time dependent manner, was detected (**Fig. 4**). The decrease of the oxidation peak G was due to a decrease of the number of free guanine residues in single-stranded oligonucleotides, the increase of the oxidation peak G_q was due to an increased number of G-quartets, and the oxidation peak G_q potential shift to more positive potentials was due to the formation and stabilisation of rigid G-quadruplexes that are more difficult oxidised.

DP voltammetry and AFM enabled the characterisation of G-rich oligonucleotides self-assembling into higher-order nanostructures, in the presence of high K^+ ions concentration and/or long incubation times, very relevant for biomedical and

nanotechnological applications [28, 40, 41].

The ability to form long G-nanowires was only found in the sequence $d(G)_{10}$ (**Figs. 4A and 4B**), but both sequences $d(G)_{10}$ and $d(TG_9)$ self-assembled into short quadruplex super-structures (**Figs. 4A–4E**), while the sequence $d(TG_8T)$ was not able to self-assemble into a quadruplex super-structure (**Figs. 4F and 4G**), due to the presence of thymine residues at both 5' and 3' ends, forming only short G-quadruplexes. Depending on the application, each one of the structures can be useful: the perfectly aligned short and compact G-quadruplexes can be used for screening cancer therapeutic agents, the perfectly aligned G-nanowires may represent building blocks of molecular nanowires for nanoelectronics and the G-based super-structures and frayed G-nanowires with slipped-strands can work as a nucleation platform for the addition of subsequent strands and the formation of larger structures.

3 G-quadruplex electrochemical biosensors

DNA electrochemical biosensors are good models for simulating nucleic acid interactions with cell membranes, potential environmental carcinogenic compounds and clarifying the mechanisms of interaction with drugs [30-35, 42]. A DNA electrochemical biosensor is based on a transducer (the electrode) with a DNA probe immobilized on its surface, the changes that occur in the DNA structure during interaction with DNA-binding molecules being translated in electrical signal.

The majority of DNA electrochemical biosensors are label-free devices, directly monitoring the changes in the oxidation peaks of the DNA guanine and adenine residues after the interaction with the analyte [30-35]. Nevertheless, to the present date, no label-free

DNA electrochemical biosensors based on direct monitoring the modifications of the G and G_q oxidation peaks have been reported, all G-quadruplex electrochemical biosensors used redox labels as amplification strategies.

3.1 G-quadruplex electrochemical aptasensors

Short aptamers that adopt G-quadruplex secondary structures received increased attention due to their specific binding to a variety of molecular targets, ranging from small ions and organic molecules to peptides, proteins, enzymes, antibodies and cell surface receptors [43, 44]. The majority of G-quadruplex electrochemical aptasensors are using thrombin binding aptamers and gold electrodes as electrochemical transducers, the aptamers attachment being achieved using amine or thiol functionalization [45-47, 48] or the affinity of biotin to avidin, streptavidin or neutravidin [49, 50].

The G-quadruplex electrochemical aptasensors can be categorized depending on the assay format, the most important being sandwich-type aptasensors (dual-site binding) and structure switching-based aptasensors (single-site binding) [51]. Small molecules are generally detected using the single-site binding configuration, while protein targets can be detected via both single-site and dual-site binding [52, 53].

3.1.1 Sandwich-type G-quadruplex electrochemical aptasensors

Sandwich-type G-quadruplex aptasensors are generally based on the aptamer ability to recognize different positions on the analyte, such as the thrombin binding aptamer recognising the fibrinogen and heparin binding sites of thrombin (aptamer–analyte–aptamer sandwich, **Scheme 3A**). The aptasensor is composed by two aptamer layers: the first

aptamer is immobilized on the electrode and is used for capturing the analyte, and the second labelled aptamer is used for electrochemical detection. The labels are either redox molecules or enzymes with catalytic activity that transform the substrate into an electroactive product.

The first reported G-quadruplex electrochemical aptasensor for thrombin had a sandwich-type format, with the first thrombin aptamer immobilized on gold and the second one labelled with pyrroquinoline quinone glucose dehydrogenase [54, 55]. The increase of the current generated by the enzyme was observed and > 10 nM thrombin was detected selectively.

Although the majority of sandwich-type G-quadruplex electrochemical aptasensors reported in the literature was using the immobilisation of the first aptamer via thiol [56- 60] or amine functionalization [61], and more recently magnetic beads [62, 63], a variety of strategies have been employed for labelling the second aptamer, such as enzymes [54-56], nanocomposites [60], nanoparticles [57, 58, 64] and quantum dots [59].

Apart from the aptamer–analyte–aptamer sandwich approach, other design strategies were also employed, consisting in either attaching the analyte to the surface via an antibody combined with a labelled G-quadruplex aptamer for detection (antibody–analyte–aptamer sandwich, **Scheme 3B**) [65], or attaching the analyte to the surface via a G-quadruplex aptamer, the detection being performed with a redox labelled antibody (aptamer–analyte– antibody sandwich, **Scheme 3C**) [61].

3.1.2 Structure-switching G-quadruplex electrochemical aptasensors

The structure-switching strategy for G-quadruplex electrochemical aptasensors is based on single-stranded to G-quadruplex conformational change of the aptamer structure

upon binding the analyte (**Scheme 4)**. This strategy generally involves the direct immobilization of the aptamer on the electrode surface, the aptamer being modified by a redox label (e.g. ferrocene or methylene blue) for signal amplification [53, 66].

The first structure-switching G-quadruplex electrochemical aptasensor used a thrombin aptamer sequence labelled with methylene blue at the 3' terminus and attached its 5' terminus to a gold electrode [53, 67]. The aptasensor detection type was signal-off (**Scheme 4**), *i.e.* the thrombin binding produced a decrease in the faradaic current of the methylene blue redox label, and the sensor was enough selective to detect thrombin directly in blood serum with a thrombin detection limit of 20 nM. Similar G-quadruplex aptasensors for thrombin were developed in parallel, using ferrocene labels [68-70]. The signal-on aptasensor achieved an increase in signal of ~300% with a saturated target and a detection limit of 3 nM [71].

Many different procedures have been used to improve the sensitivity of the G-quadruplex electrochemical aptasensors using amplification strategies based on redox labels, such as ferrocene [72-80] or methylene blue [81-83], $Ru(NH_3)_6]^{3+}$ [84], electrochemical active-inactive switch between monomer/dimer forms of carminic acid [85] or catalysts such as horseradish peroxidase [86]. Nanoparticle-based materials were also used as signal amplification strategies for ultrasensitive electrochemical aptasensing, including gold, platinum [57] and Fe_3O_4 nanoparticles [87] and quantum dot-coated silica nanospheres [88]. Apart from gold electrodes, only recently other electrochemical

transducers have been employed, such as modified platinum [89] or carbon electrodes [64, 76, 89-92].

Based on the aptamer conformational change in the presence of K^+, different electrochemical aptasensors has been developed for selective potassium recognition. The formation of a G-quadruplex structure in the presence of K^+ ions was detected by monitoring the changes on the electron transfer between a redox label and the electrode surface [93- 95], or by detecting the changes on the interfacial electron transfer resistance [96]. The same strategy was used for specific recognition of other metal ions, such as Tb^{3+} [97].

Taking advantage of the ability of thrombin to catalyze the hydrolysis of the peptide (-Ala-Gly-Arg-*p*-nitroaniline) to *p*-nitroaniline, bound thrombin was also electrochemically detected, by quantifying the p-nitroaniline reaction product [56].

Another strategy for G-quadruplex electrochemical aptasensors used a non-specific immobilization of the protein on the electrode surface and electrochemical detection with a labelled G-quadruplex aptamer. In this approach, thrombin was detected with using horseradish peroxidase label, allowing a detection limit of 3.5 nM, sufficient for clinical diagnosis of metastatic lung cancer, where the concentration of thrombin level achieved is 5.4 nM [56].

3.2 Hemin/G-quadruplex DNAzymes electrochemical biosensors

Hemin/G-quadruplex peroxidase-mimicking DNAzymes, which consist in G-quadruplex sequences with intercalated hemin molecules, have recently attract great interest in biosensor [98, 99] and biofuel cell technologies [100]. Hemin is an iron-

containing porphyrin whose peroxidase activity increases in the presence of DNA, facilitating the redox reaction between a target molecule (the substrate, *e.g.* 3,3′,5,5′-tetramethylbenzidine, hydroquinone or ferrocene methyl alcohol) and H_2O_2, which results in the appearance of an oxidized target molecule (the product), that is electrochemically detected (**Scheme 5)**.

Hemin/G-quadruplex DNAzymes electrochemical biosensors can be used to follow the activity of glucose oxidase [101, 102], the simplest methodology consisting on attaching glucose oxidase to the electrode surface through a nucleic acid sequence able to form a G-quadruplex structures in the presence of hemin. The glucose oxidase mediates the glucose oxidation to gluconic acid and H_2O_2 and the resulting H_2O_2 is analysed through its electrocatalysed reduction by the DNAzyme.

Hemin/G-quadruplex DNAzymes electrochemical biosensors can also be successfully used for the detection of proteins [103-105] or low-molecular-weight molecules, such as adenosine monophosphate (AMP) [101, 106], anticancer drugs [107], gaseous ligands [108], toxins [109, 110], pollutant agents [111] or metal ions [112, 113]). The most common strategy consists on modification of the gold electrode by a hairpin nucleic acid oligonucleotide that contains both a sequence capable to form G-quadruplex and an aptamer able to specifically bind the analyte. In the presence of the analyte and hemin, the hairpin structures are opened, the analyte binds to the aptamer part, and hemin/G-quadruplex structures are formed on the electrode surface.

Later on, more complicated strategies have been proposed to improve the sensitivity of hemin/G-quadruplex DNAzymes electrochemical biosensors, such as dual-amplification [114], background noise reduction [115] or autocatalytic target recycling strategies [116].

A different design for hemin/G-quadruplex DNAzymes electrochemical biosensors take advantage of the hemin/G-quadruplex acting both as a NADH oxidase, assisting the oxidation of NADH to NAD^+ together with the generation of H_2O_2 in the presence of dissolved O_2, as well as a hemin/G-quadruplex DNAzyme to bioelectrocatalyse the reduction of the produced H_2O_2 [117-119].

4 Conclusion

This review is focused on key features of the G-quadruplex nucleic acid electrochemistry and their application in G-quadruplex-based electrochemical biosensor devices, such as G-quadruplex aptasensors and hemin/G-quadruplex peroxidase-mimicking DNAzymes biosensors. So far no label-free DNA electrochemical biosensors, based on direct monitoring the modifications of the G and G_q oxidation peaks, have been reported, and all G-quadruplex electrochemical biosensors are using redox labels as amplification strategies.

The detailed knowledge of G-quadruplex formation mechanism is extremely important for the design and fabrication of quadruplex-based therapeutic agents in medicine or nanostructures in nanotechnology. Voltammetric techniques were successfully employed to study the transformation of single-strand sequences into G-quadruplexes or G-based nanostructures, in freshly prepared solutions, for concentrations 10 times lower than usually detected by other techniques, such as UV absorbance, circular dichroism or electrospray mass spectroscopy. The voltammetric results demonstrated that the appropriate choice of the oligonucleotide sequence base composition, monovalent cation concentration and incubation time, can lead to the formation of different G-based nanostructures, extremely

important for the design and fabrication of future non-mediated (label free) nanostructured DNA electrochemical biosensor devices.

Acknowledgements

Financial support from Fundação para a Ciência e Tecnologia (FCT), projects PTDC/QUI-QUI/098562/2008, PTDC/SAU-BMA/118531/2010, PTDC/QEQ-MED/0586/2012 and PEst-C/EME/UI0285/2013, POPH (co-financed by the European Community Funds FSE and FEDER/COMPETE– Programa Operacional Factores de Competitividade), is gratefully acknowledged.

References

[1] T. Simonsson, G-quadruplex DNA structures - variations on a theme, Biol. Chem. 382 (2001) 621.

[2] J.L. Huppert, S. Balasubramanian, Prevalence of quadruplexes in the human genome, Nucleic Acid. Res. 33 (2005) 2908.

[3] A.K. Todd, M. Johnston, S. Neidle, Highly prevalent putative quadruplex sequence motifs in human DNA, Nucleic Acid. Res. 33 (2005) 2901.

[4] S. Burge, G.N. Parkinson, P. Hazel, A.K. Todd, S. Neidle, Quadruplex DNA: Sequence, topology and structure, Nucleic Acid. Res. 34 (2006) 5402.

[5] S. Neidle, S. Balasubramanian (Eds.), Quadruplex Nucleic Acids, The Royal Society of Chemistry, Cambridge, UK, 2006.

[6] J.L. Huppert, Hunting G-quadruplexes, Biochimie 90 (2008) 1140.

[7] M.M. Dailey, C. Hait, P.A. Holt, J.M. Maguire, J.B. Maier, M.C. Miller, L. Petraccone, J.O. Trent Structure-based drug design: from nucleic acid to membrane protein targets experimental and molecular pathology, Exp. Mol. Pathol. 86 (2009) 141.

[8] C. Punchihewa, D. Yang, Therapeutic targhet and drugs II: G-quadruplex and G-quadruplex inhibitors, in K. Hiyama (Ed.), Telomeres and telomerase in cancer, Ch. 11, Humana Press, Springer, 2009, p. 251.

[9] S. Neidle, The structures of quadruplex nucleic acids and their drug complexes, Curr. Opin. Struct. Biol. 19 (2009) 239.

[10] K. Hiyama (Ed.), Telomeres and telomerase in cancer, Humana Press, New York, 2009.

[11] M.J. Giraud-Panis, S. Pisano, A. Poulet, M.H. Le Du, E. Gilson, Structural identity of telomeric complexes, FEBS Letters 584 (2010) 3785.

[12] H. Wang, G.J. Nora, H. Ghodke, P.L. Opresko, Single molecule studies of physiologically relevant telomeric tails reveal POT1 mechanism for promoting G-quadruplex unfolding, J. Biol. Chem. 286 (2010) 7479.

[13] S. Neidle, DNA and RNA quadruplex structures, in S. Neidle (Ed.), Therapeutic applications of quadruplex nucleic acids, Ch. 2, Academic Press, Boston, 2012, p. 21.

[14] J.L. Mergny, A. Cian, A. Ghelab, B. Sacca, L. Lacroix, Kinetics of tetramolecular quadruplexes, Nucleic Acids Res. 33 (2005) 81.

[15] P.L. Tran, A. de Cian, J. Gros, R. Moriyama, J.L. Mergny, Tetramolecular quadruplex stability and assembly, Top. Curr. Chem. (2013) 243.

[16] N. Borovok, N. Iram, D. Zikich, J. Ghabboun, G.I. Livshits, D. Porath, A. B. Kotlyar, Assembling of G-strands into novel tetra-molecular parallel G4-DNA nanostructures using avidin-biotin recognition, Nucleic Acids Res. 36 (2008) 5050.

[17] Borovok, Tatiana Molotsky, Jamal Ghabboun, Danny Porath, Alexander Kotlyar, Efficient procedure of preparation and properties of long uniform G4–DNA nanowires, Anal. Biochem. 374 (2008) 71.

[18] E. Shapir, L. Sagiv, N. Borovok, T. Molotski, A. B. Kotlyar, D. Porath, High-resolution STM imaging of novel single G4-DNA molecules, J. Phys. Chem. B 112 (2008) 9267.

[19] M. Biyani, K. Nishigaki, Structural characterization of ultra-stable higher-ordered aggregates generated by novel guanine-rich DNA sequences, Gene 364 (2005) 130.

[20] T.C. Marsh, J. Vesenka, E. Henderson, A new DNA nanostructure, the G-wire, imaged by scanning probe microscopy, Nucleic Acids Res. 23 (1995) 696.

[21] J. Vesenka, AFM of guanine rich oligonucleotide surface structures, in: W. Fritzsche, L. Spindler (Eds.) Guanine quartets – structure and application, Ch. 2, RCS publishing, Cambridge, UK, 2013, p. 110.

[22] J.E. Johnson, J. S. Smith, M.L. Kozak, F.B. Johnson, In vivo veritas: Using yeast to probe the biological functions of G-quadruplexes, Biochimie, 90 (2008) 1250.

[23] O.I. Wilner, I. Willner, Functionalized DNA nanostructures, Chem. Rev. 112 (2012) 2528.

[24] D. Sun, L.H. Hurley, Biochemical Techniques for the Characterization of G-Quadruplex Structures: EMSA, DMS Footprinting, and DNA Polymerase Stop Assay, Methods Mol. Biol. 608 (2010) 65.

[25] J. Jaumot, R. Gargallo, Experimental methods for studying the interactions between G-quadruplex structures and ligands, Curr. Pharm. Des. 18 (2012) 1900.

[26] M. Adrian, B. Heddi, A.T. Phan, NMR spectroscopy of G-quadruplexes, Methods 57 (2012) 11.

[27] A.I. Karsisiotis, M. Webba da Silva, Structural probes in quadruplex nucleic acid structure determination by NMR, Molecules 17 (2012) 13073.

[28] A.-M. Chiorcea-Paquim, P. Santos,V.C. Diculescu, R. Eritja, A.M. Oliveira-Brett, Electrochemical characterization of guanine quadruplexes, in: W. Fritzsche, L. Spindler (Eds.) Guanine quartets – structure and application, Ch. 2, RCS publishing, Cambridge, UK, 2013, p. 100.

[29] A.M. Oliveira Brett, S.H.P. Serrano, J.A.P. Piedade, Electrochemistry of DNA, in: R.G. Compton (Ed.), Comprehensive Chemical Kinetics, Applications of Kinetic Modelling, Vol. 37, Ch. 3, Elsevier, Amsterdam, 1999, 91.

[30] A.M. Oliveira Brett, DNA-based biosensors, in: L. Gorton (Ed.), Biosensors and Modern Biospecific Analytical Techniques, Comprehensive Analytical Chemistry Vol. XLIV (Series Ed. D. Barceló), Ch. 4, Elsevier, Amsterdam, 2005, p. 179.

[31] A.M. Oliveira Brett, Electrochemistry for probing DNA damage, in: C.A. Grimes, E.C. Dickey, M.V. Pishko (Eds.), Encyclopedia of Sensors, Vol. 3, American Scientific Publishers, USA, 2006, p. 301.

[32] A.M. Oliveira Brett, A.–M. Chiorcea–Paquim, V.C. Diculescu, J.A.P. Piedade, Electrochemistry of nanoscale DNA surface films on carbon, Med. Eng. Phys. 28 (2006) 963.

[33] A.M. Oliveira Brett, V. Diculescu, A.M. Chiorcea-Paquim, S.H.P. Serrano, DNA-electrochemical biosensors for investigating DNA damage, in: S. Alegret and A. Merkoçi (Eds.), Comprehensive Analytical Chemistry (CAC), Vol. 49, Electrochemical Sensor analysis (ECSA), Sec. F. Biosensors, Elsevier, Amsterdam, The Netherlands, 2007, Ch. 20, p. 413, Proc. 28, e203-e205, Proc. 29, e207-e211,2007.

[34] Ana Maria Oliveira Brett, Electrochemical DNA Assays, in: P.N Bartlett (Ed.), Bioelectrochemistry: Fundamentals, Experimental Techniques and Applications, Ed, Ch. 12, John Wiley, UK, 2008, p. 411.

[35] A.M. Oliveira Brett, Nanobioelectrochemistry, in: D.J. Lockwood, P. Schmuki and S. Virtanen (Eds.), Electrochemistry at the Nanoscale, Nanostrutures Science and Technology, Series, Ch. 11, Springer Science Publishing, 2009, p. 407.

[36] V. C. Diculescu, A.-M. Chiorcea-Paquim, R. Eritja, A. M. Oliveira-Brett, Thrombin-binding aptamer quadruplex formation: AFM and voltammetric characterization, Journal of Nucleic Acids (2010) article ID 841932, 8 pages, doi:10.4061/2010/8419321.

[37] C. M. A. Brett, A. M. Oliveira Brett, S. H. P. Serrano, On the adsorption and electrochemical oxidation of DNA at glassy carbon electrodes, J. Electroanal. Chem. 366 (1994) 225.

[38] R.F. Macaya, P. Schultze, F.W. Smith, J.A. Roe, J. Feigon, Thrombin-binding DNA aptamer forms a unimolecular quadruplex structure in solution, Proc. Natl. Acad. Sci. USA 90 (1993) 3745.

[39] V.C. Diculescu, A.-M. Chiorcea-Paquim, R. Eritja, A.M. Oliveira-Brett, Evaluation of the structure-activity relationship of thrombin binding aptamers by voltammetry and atomic force microscopy, J. Electroanal. Chem. 656 (2011) 159.

[40] A.-M. Chiorcea-Paquim, P. Santos,V.C. Diculescu, R. Eritja, A.M. Oliveira-Brett, Self-assembled G-quadruplex nanostructures: AFM and voltammetric characterization. Phys. Chem. Chem. Phys. 15 (2013) 9117.

[41] A.-M. Chiorcea-Paquim, P. Santos,V.C. Diculescu, A.M. Oliveira-Brett, Atomic force microscopy and voltammetric characterisation of synthetic homo-oligodeoxynucleotides, Electrochim. Acta 2013, in press.

[42] V.C. Diculescu, A.–M. Chiorcea-Paquim, A.M. Oliveira Brett, Electrochemical DNA sensors for detection of DNA damage, Sensors 5 (2005) 377.

[43] D. Musumeci, D. Montesarchio, Polyvalent nucleic acid aptamers and modulation of their activity: a focus on the thrombin binding aptamer, Pharmacol. Therapeut. 136 (2012) 202.

[44] T. Hianik, J. Wang, Electrochemical Aptasensors – Recent achievements and perspectives, Electroanal. 21 (2009) 1223.

[45] A.K.H. Cheng, D. Sen, H.Z. Yu,Design and testing of aptamer-based electrochemical biosensors for proteins and small molecules, Bioelectrochemistry 77 (2009) 1.

[46] M.N. Velasco-Garcia, S. Missailidis, New trends in aptamer-based electrochemical biosensors, Gene Ther. Mol. Biol. 13 (2009) 1.

[47] X.B. Yin, Functional nucleic acids for electrochemical and electrochemiluminescent sensing applications, TrAC-Trend. Anal. Chem. 33 (2012) 81.

[48] E.E. Ferapontova, K.V. Gothelf, Recent Advances in Electrochemical Aptamer-Based Sensors, Curr. Org. Chem. 15 (2011) 498.

[49] T. Hianik, V. Ostatná, M. Sonlajtnerova, I. Grman, Influence of ionic strength, pH and aptamer configuration for binding affinity to thrombin, Bioelectrochemistry, 70 (2007) 127.

[50] T. Hianik, DNA/RNA aptamers: novel recognition structures in biosensing, in: S. Alegret and A. Merkoçi (Eds), Comprehensive Analytical Chemistry, Elsevier, Ch. 33, Vol. 49, 2007, p. 801.

[51] J. Liu, Z. Cao, Y. Lu, Functional Nucleic Acid Sensors, Chem. Rev. 109 (2009) 1948.

[52] S. Song, L. Wang, J. Li, C. Fan, J. Zhao, Aptamer-based biosensors, TrAC-Trend. Anal. Chem. 27 (2008) 108.

[53] A.A. Lubin, K.W Plaxco, Folding-Based Electrochemical Biosensors: The Case for responsive nucleic acid architectures, Acc. Chem. Res. 43 (2010) 4496.

[54] K. Ikebukuro, C. Kiyohara, K. Sode, Electrochemical detection of protein using a double aptamer sandwich, Anal. Lett. 37 (2004) 2901.

[55] K. Ikebukuro, C. Kiyohara, K. Sode, Novel electrochemical sensor system for protein using the aptamers in sandwich manner, Biosens. Bioelectron. 20 (2005) 2168.

[56] M. Mir, M. Vreeke, I. Katakis Different strategies to develop an electrochemical thrombin aptasensor, Electrochem. Comm. 8 (2006) 505.

[57] R. Polsky, R. Gill, L. Kaganovsky, I. Willner, Nucleic acid-functionalized Pt nanoparticles: Catalytic labels for the amplified electrochemical detection of biomolecules, Anal. Chem. 78 (2006) 2268.

[58] A. Numnuam, K.Y. Chumbimuni-Torres, Y. Xiang, R. Bash, P. Thavarungkul, P. Kanatharana, E. Pretsch, J. Wang, E. Bakker, Aptamer-based potentiometric measurements of proteins using ion-selective microelectrodes, Anal. Chem. 80 (2008) 707.

[59] H. Yang, J. Ji, Y. Liu, J. Kong, B. Liu, An aptamer-based biosensor for sensitive thrombin detection, Electrochem. Commun. 11 (2009) 38.

[60] K. Peng, H. Zhao, X. Wu, Y. Yuan, R. Yuan, Ultrasensitive aptasensor based on graphene-3,4,9,10-perylenetetracarboxylic dianhydride as platform and functionalized hollow PtCo nanochains as enhancers, Sensor Actuat. B- Chem. 169 (2012) 88.

[61] Md.A. Rahman, J.I. Son, M.-S. Won, Y.-B. Shim, Gold Nanoparticles Doped Conducting Polymer Nanorod Electrodes: Ferrocene catalyzed aptamer-based thrombin immunosensor, Anal. Chem. 81 (2009) 6604.

[62] S. Centi, S. Tombelli, M. Minunni, M. Mascini, Aptamer-based detection of plasma proteins by an electrochemical assay coupled to magnetic beads, Anal. Chem. 79 (2007) 1466.

[63] S. Centi, G. Messina, S. Tombelli, I. Palchetti, M. Mascini, Different approaches for the detection of thrombin by an electrochemical aptamer-based assay coupled to magnetic beads, Biosens. Bioelectron. 23 (2008) 1602.

[64] B.L. Li, Y.L. Wang, H. Wei, S.J. Dong, Amplified electrochemical aptasensor taking AuNPs, based sandwich sensing platform as a model, Biosens. Bioelectron. 23 (2008) 965.

[65] Y. Kang, K.-J. Feng, J.-W. Chen, J.-H. Jiang, G.-L. Shen, R.-Q. Yu, Electrochemical detection of thrombin by sandwich approach using antibody and aptamer, Bioelectrochemistry 73 (2008) 76.

[66] K.W. Plaxco, H.T. Sohb, Switch based biosensors: a new approach towards real-time, in vivo molecular detection, Trends Biotechnol. 29 (2011) 1.

[67] Y. Xiao, A.A. Lubin, A.J. Heeger, K.W. Plaxco, Label-free electronic detection of thrombin in blood serum by using an aptamer-based sensor, Angew. Chem. Int. Ed. 44 (2005) 5456.

[68] A. Radi, J.L.A. Sanchez, E. Baldrich, C.K. O'Sullivan, Reusable Impedimetric Aptasensor, Anal. Chem. 77 (2005) 6320.

[69] A. Radi, J.L.A. Sanchez, E. Baldrich, C.K. O'Sullivan, Reagentless, reusable, ultrasensitive electrochemical molecular beacon aptasensor, J. Am. Chem. Soc. 128 (2006) 117.

[70] J.L.A. Sanchez, E. Balrich, A.E. Radi, S. Dondapati, P.L. Sanchez, I. Katakis, C.K. O'Sullivan, Electronic 'Off-On' molecular switch for rapid detection of thrombin, Electroanal. 18 (2006) 1957.

[71] Y. Xiao, B.D. Piorek, K.W. Plaxco, A.J. Heeger, A reagentless signal-on architecture for electronic, aptamer-based sensors via target-induced strand displacement. J. Am. Chem. Soc. 127 (2005) 17990.

[72] M. Mir, A. Toby, A. Jenkins, I. Katakis, Ultrasensitive detection based on an aptamer beacon electron transfer chain, Electrochem. Commun. 10 (2008) 1533.

[73] X. Li, L. Shen, D. Zhang, H. Qi, Q. Gao, F. Ma, C. Zhang, Electrochemical impedance spectroscopy for study of aptamer–thrombin interfacial interactions, Biosens. Bioelectron 23 (2008) 1624.

[74] Z. Zhang, W. Yang, J. Wang, C. Yang, F. Yang, X. Yang, A sensitive impedimetric thrombin aptasensor based on polyamidoamine dendrimer, Talanta, 78 (2009) 1240.

[75] J. Chen, J. Zhang, J. Li, H.H. Yang, F. Fu, G. Chen, An ultrasensitive signal-on electrochemical aptasensor via target-induced conjunction of split aptamer fragments, Biosens. Bioelectron. 25 (2010) 996.

[76] X. Liu, Y. Li, J. Zheng, J. Zhang, Q. Sheng, Carbon nanotube-enhanced electrochemical aptasensor for the detection of thrombin, Talanta 81 (2010) 1619.

[77] G. Castillo, I. Lamberti, L. Mosiello, T. Hianik, Impedimetric DNA aptasensor for sensitive detection of ochratoxin A in food, Electroanal. 24 (2012) 512.

[78] N. Meini, C. Farre, C. Chaix, R. Kherrat, S. Dzyadevych, N. Jaffrezic-Renault, A sensitive and selective thrombin impedimetric aptasensor based on tailored aptamers obtained by solid-phase synthesis, Sens. Actuat. B- Chem. 166–167 (2012) 715.

[79] A. Hayat, S. Andreescu, J.L. Marty, Design of PEG-aptamer two piece macromolecules as convenient and integrated sensing platform: Application to the label free detection of small size molecules, Biosens. Bioelectron. 45 (2013) 168.

[80] Y. Jalit, F.A. Gutierrez, G. Dubacheva, C. Goyer, L. Coche-Guerente, E. Defrancq, P. Labbé, G.A. Rivas, M.C. Rodríguez, Characterization of a modified gold platform for the development of a label-free anti-thrombin aptasensor, Biosens. Bioelectron. 41 (2013) 424.

[81] G. Sook Bang, S. Cho, B.-G. Kim, A novel electrochemical detection method for aptamer biosensors, Biosens. Bioelectron. 21 (2005) 863.

[82] F. Yan, F. Wang, Z. Chen, Aptamer-based electrochemical biosensor for label-free voltammetric detection of thrombin and adenosine, Sens. Actuat. B-Chem. 160 (2011) 1380.

[83] H.-Y. Bai, F. Javier Del Campo, Y.-C. Tsai, Sensitive electrochemical thrombin aptasensor based on gold disk microelectrodearrays, Biosens. Bioelectron. 42 (2013) 17.

[84] A. De Rache, I. Kejnovská, M. Vorlíčková, C. Buess-Herman, Elongated thrombin binding aptamer: a G-quadruplex cation-sensitive conformational switch, Chem. Eur. J. 18 (2012) 4392.

[85] G. Cheng, B. Shen, F. Zhang, J. Wu, Y. Xu, P. He, Y. Fang, A new electrochemically active–inactive switching aptamer molecular beacon to detect thrombin directly in solution, Biosens. Bioelectron. 25 (2010) 2265.

[86] J. Zhang, J. Chen, X. Zhang, Z. Zeng, M. Chen, S. Wang, An electrochemical biosensor based on hairpin-DNA aptamer probe and restriction endonuclease for ochratoxin A detection, Electrochem. Commun. 25 (2012) 5.

[87] S. Zhang, G. Zhou, X. Xu, L. Cao, G. Liang, H. Chen, B. Liu, J. Kong, Development of an electrochemical aptamer-based sensor with a sensitive Fe_3O_4 nanopaticle-redox tag for reagentless protein detection, Electrochem. Commun. 13 (2011) 928.

[88] Y. Li, L. Deng, C. Deng, Z. Nie, M. Yang, S. Si, Simple and sensitive aptasensor based on quantum dot-coated silica nanospheres and the gold screen-printed electrode, Talanta 99 (2012) 637.

[89] H. Xu, k. Gorgy, C. Gondran, A. Le Goff, N. Spinelli, C. Lopez, E. Defrancq, S. Cosnier, Label-free impedimetric thrombin sensor based on poly(pyrrole-nitrilotriacetic acid)-aptamer film, Biosens. Bioelectron. 41 (2013) 90.

[90] E. Suprun, V. Shumyantseva, T. Bulko, S. Rachmetova, S. Rad'ko, N. Bodoev, A. Archakov, Au-nanoparticles as an electrochemical sensing platform for aptamer–thrombin interaction, Biosens. Bioelectron. 24 (2008) 825.

[91] L. Feng, Y. Chen, J. Ren, X. Qu, A graphene functionalized electrochemical aptasensor for selective label-free detection of cancer cells, Biomaterials, 32, (2011) 2930.

[92] M.Y. Elahi, S.Z. Bathaie, M.F. Mousavi, R. Hoshyar, S. Ghasemi, A new DNA-nanobiosensor based on G-quadruplex immobilized on carbon nanotubes modified glassy carbon electrode, Electrochim. Acta 82 (2012) 143.

[93] A.E. Radi, C.K. O'Sullivan, Aptamer conformational switch as sensitive electrochemical biosensor for potassium ion recognition, Chem. Commun. 32 (2006) 3432.

[94] Z.S. Wu, C.R. Chen, G.L. Shen, R.Q. Yu, Reversible electronic nanoswitch based on DNA G quadruplex conformation: a platform for single-step, reagentless potassium detection, Biomaterials 29 (2008) 2689.

[95] J. Zhang, Y. Wan, L. Wang, S. Song, D. Li, C. Fan, Switchable charge transport path via a potassium ions promoted conformational change of G-quadruplex probe monolayer, Electrochem. Commun., 10 (2008) 1258.

[96] Z. Chen, L. Chen, H. Ma, T. Zhou, X. Li, Aptamer biosensor for label-free impedance spectroscopy detection of potassium ion based on DNA G-quadruplex conformation, Biosens. Bioelectron. 48 (2013) 108.

[97] J. Zhang, J.H. Chena, R. Chen, G. Chen, F. Fu, An electrochemical biosensor for ultratrace terbium based on Tb3+ promoted conformational change of human telomeric G-quadruplex, Biosens. Bioelectron. 25 (2009) 378.

[98] J. Kosman, B. Juskowiak, Peroxidase-mimicking DNAzymes for biosensing applications: A review, Anal. Chim. Acta 707 (2011) 7.

[99] N. Kaneko, K. Horii, S. Kato, J. Akitomi, I. Waga, High-throughput quantitative screening of peroxidase-mimicking DNAzymes on a microarray by using electrochemical detection, Anal. Chem. (2013) in press, doi: 10.1021/ac4002518.

[100] M. Zhang, S. Xu, S.D. Minteer, D.A. Baum, Investigation of a deoxyribozyme as a biofuel cell catalyst, J. Am. Chem. Soc. 133 (2011) 15890.

[101] G. Pelossof, R. Tel-Vered, J. Elbaz, I. Willner, Amplified biosensing using the horseradish peroxidase-mimicking DNAzyme as an electrocatalyst, Anal. Chem. 82 (2010) 4396.

[102] L. Bai, R. Yuan, Y. Chai, Y. Yuan, Y. Zhuo, L. Mao, Bi-enzyme functionlized hollow PtCo nanochains as labels for an electrochemical aptasensor, Biosens. Bioelectron. 26 (2011) 4331.

[103] D. Li, B. Shlyahovsky, J. Elbaz, I. Willner, Amplified analysis of low-molecular-weight substrates or proteins by the self-assembly of DNAzyme-aptamer conjugates, J. Am. Chem. Soc. 129 (2007) 5804.

[104] K. Zhang, X. Zhu, J. Wang, L. Xu, G. Li, Strategy to fabricate an electrochemical aptasensor: application to the assay of adenosine deaminase activity, Anal. Chem. 82 (2010) 3207.

[105] N. Yang, Y. Cao, P. Han, X. Zhu, L. Sun, G. Li, Tools for investigation of the RNA endonuclease activity of mammalian Argonaute2 protein, Anal. Chem. 84(2012) 84 2492.

[106] L. Liu, Z. Liang, Y. Li, Label free, highly sensitive and selective recognition of small molecule using gold surface confined aptamers, Solid State Sci. 14 (2012) 1060.

[107] Q. Yang, Y. Nie, X. Zhu, X. Liu, G. Li, Study on the electrocatalytic activity of human telomere G-quadruplex–hemin complex and its interaction with small molecular ligands, Electrochim. Acta 55 (2009) 276.

[108] X. Zhu, W. Zhang, H. Xiao, J. Huang, G. Li, Electrochemical study of a hemin–DNA complex and its activity as a ligand binder, Electrochim. Acta 53 (2008) 4407.

[109] Y. Zhu, L. Xu, W. Ma, W. Chen, W. Yan, H. Kuang, L. Wang, C. Xu, G-quadruplex DNAzyme-based microcystin-LR (toxin) determination by a novel immunosensor, Biosens. Bioelectron. 26 (2011) 4393.

[110] C. Yang, V. Lates, B. Prieto-Simón, J.L. Marty, X. Yang, Aptamer-DNAzyme hairpins for biosensing of Ochratoxin A, Biosens. Bioelectron. 32 (2012) 208.

[111] G. Liang, X. Liu, X. Li, Highly sensitive detection of α-naphthol based on G-DNA modified gold electrode by electrochemical impedance spectroscopy, Biosens. Bioelectron. 45 (2013) 46.

[112] G. Pelossof, R. Tel-Vered, I. Willner, Amplified surface plasmon resonance and electrochemical detection of Pb^{2+} ions using the Pb^{2+}-dependent DNAzyme and hemin/G-quadruplex as a label, Anal. Chem. 84 (2012) 3703.

[113] Z. Zhang, J. Yin, Z. Wu, R. Yu, Electrocatalytic assay of mercury(II) ions using a bifunctional oligonucleotide signal probe, Anal. Chim. Acta 762 (2013) 47.

[114] Y. Yuan, X. Gou, R. Yuan, Y. Chai, Y. Zhuo, L. Mao, X. Gan, Electrochemical aptasensor based on the dual-amplification of G-quadruplex horseradish peroxidase-mimicking DNAzyme and blocking reagent-horseradish peroxidase, Biosens. Bioelectron. 26 (2011) 4236.

[115] B. Jiang, M. Wang, C. Li, J. Xie, Label-free and amplified aptasensor for thrombin detection based on background reduction and direct electron transfer of hemin, Biosens. Bioelectron. 43 (2013) 289.

[116] S. Liu, C. Wang, C. Zhang, Y. Wang, B. Tang, Label-free and ultrasensitive electrochemical detection of nucleic acids based on autocatalytic and exonuclease III-assisted target recycling strategy, Anal. Chem. 85 (2013) 2282.

[117] S. Xie, Y. Chai, R. Yuan, L. Bai, Y. Yuan, Y. Wang, A dual-amplification aptasensor for highly sensitive detection of thrombin based on the functionalized graphene-Pd nanoparticles composites and the hemin/G-quadruplex, Anal. Chim. Acta 755 (2012) 46.

[118] Y. Yuan, R. Yuan, Y. Chai, Y. Zhuo, X. Ye, X. Gana, L. Baia, Hemin/G-quadruplex simultaneously acts as NADH oxidase and HRP-mimicking DNAzyme for simple, sensitive pseudobienzyme electrochemical detection of thrombin, Chem. Commun. 48 (2012) 4621.

[119] Y. Yuan, G. Liu, R. Yuan, Y. Chai, X. Gan, L. Bai, Dendrimer functionalized reduced graphene oxide as nanocarrier for sensitive pseudobienzyme electrochemicalaptasensor, Biosens. Bioelectron. 42 (2013) 474.

Figures

Scheme 1 (A) Chemical structure of guanine (G) base. (B) G-quartet (G_q) showing the hydrogen bonding between four planar G bases. (C) Schematic representation of tetramer, dimer and monomer G-quadruplexes composed by three staked G-quartets; the cations that stabilise the G-quadruplexes are shown as black balls.

Scheme 2 Schematic representation of unimolecular antiparallel G-quadruplex structures formed by the thrombin binding aptamers: (A) 5'-GGTTGGTGTGGTTGG-3' (TBA) and (B) 5'-GGGTTGGGTGTGGGTTGGG-3' (eTBA).

Scheme 3 Sandwich-type quadruplex aptasensors. (A) Aptamer–analyte–aptamer sandwich: the first aptamer is used for binding the analyte to the surface and the second labelled aptamer is used for detection. (B) Antibody–analyte–aptamer sandwich: the analyte is bound to the surface via an antibody and a labelled aptamer is used for detection; (C) Aptamer–analyte–antibody sandwich: the analyte is bound to the surface via an aptamer and a labelled antibody is used for detection.

Scheme 4 Structure-switching quadruplex aptasensors; the analyte binding causes the aptamer conformational modifications and increases the distance from the redox label to the electrode.

Scheme 5 Hemin/G-quadruplex peroxidase-mimicking DNAzymes electrochemical biosensor.

Fig. 1 (A, D) DP voltammograms baseline corrected, in 0.1 M NaH_2PO_4/Na_2HPO_4 buffer solution pH = 7.0, with 1 μg mL^{-1} (A) TBA and (D) eTBA, (▬) in the absence and in the presence of 100 mM K^+, (▬) 0 h and (•••) 24 h incubation. (B, C, E, F) AFM images of (B, C) TBA and (E, F) eTBA spontaneously adsorbed during 3 min, from solutions of 1 μg mL^{-1} TBA or eTBA in 0.1 M NaH_2PO_4/Na_2HPO_4 buffer solution pH = 7.0, (B, E) in the absence and (C, F) in the presence of 100 mM K^+, 24 h incubation. [Adapted from reference [28] with permission].

Fig. 2 (A, B, D, E) AFM images of complex (A, B) TBA–thrombin and (D, E) eTBA–thrombin, spontaneously adsorbed during 5 min from incubated solutions, in 0.1 M NaH_2PO_4/Na_2HPO_4 buffer solution pH = 7.0, of 1 μg mL^{-1} TBA or eTBA with 10 μg mL^{-1} thrombin, (A, D) in the absence and (B, E) in the presence of 100 mM K^+, 24 h of incubation. (C, F) DP voltammograms baseline corrected, in 0.1 M NaH_2PO_4/Na_2HPO_4 buffer solution pH = 7.0, with 1 μg mL^{-1} thrombin incubated with 1 μg mL^{-1} (C) TBA and (F) eTBA, in the absence of K^+, (▬) 0 h and (•••) 48 h incubation, and in the presence of 100 mM K^+, (▬) 0 h and (•••) 48 h incubation. [Adapted from reference [28] with permission].

Fig. 3 (A) DP voltammograms baseline corrected in 3.0 μM $d(G)_{10}$, in 0.1 M NaH_2PO_4/Na_2HPO_4 buffer solution pH = 7.0, in the absence of K^+, (▪●▪) 0 h,

(●●●) 24 h, (▪▪▪) 48 h and (▬) 14 days incubation, and in the presence of 1 mM K^+ (▪▪▪) 0 h and (▬) 24 h incubation. (B, C) AFM images of $d(G)_{10}$ spontaneous adsorbed from 0.3 μM $d(G)_{10}$, in 0.1 M NaH_2PO_4/Na_2HPO_4 buffer solution pH = 7.0, (B) 0 h and (C) 14 days incubation. [Adapted from reference [40] with permission].

Fig. 4 (A, D, F) DP voltammograms baseline corrected, in 0.1 M NaH_2PO_4/Na_2HPO_4 buffer solution pH = 7.0, with 3.0 μM (A) $d(G)_{10}$, (D) $d(TG_9)$ and (F) $d(TG_8T)$, (▪▪▪) in the absence and in the presence of (▬) 5 mM, (●●●) 50 mM, (▪●▪) 100 mM, (▪▪▪) 200 mM and (▬) 1 M K^+, after 0 h incubation. (B, C, E, G) AFM images of (B, C) $d(G)_{10}$, (E) $d(TG_9)$ and (G) $d(TG_8T)$ spontaneous adsorbed from 0.3 μM $d(G)_{10}$, $d(TG_9)$ or $d(TG_8T)$, in 0.1 M NaH_2PO_4/Na_2HPO_4 buffer solution pH = 7.0, in the presence of 200 mM K^+ ions, 24 h incubation. [Adapted from reference [40] with permission].

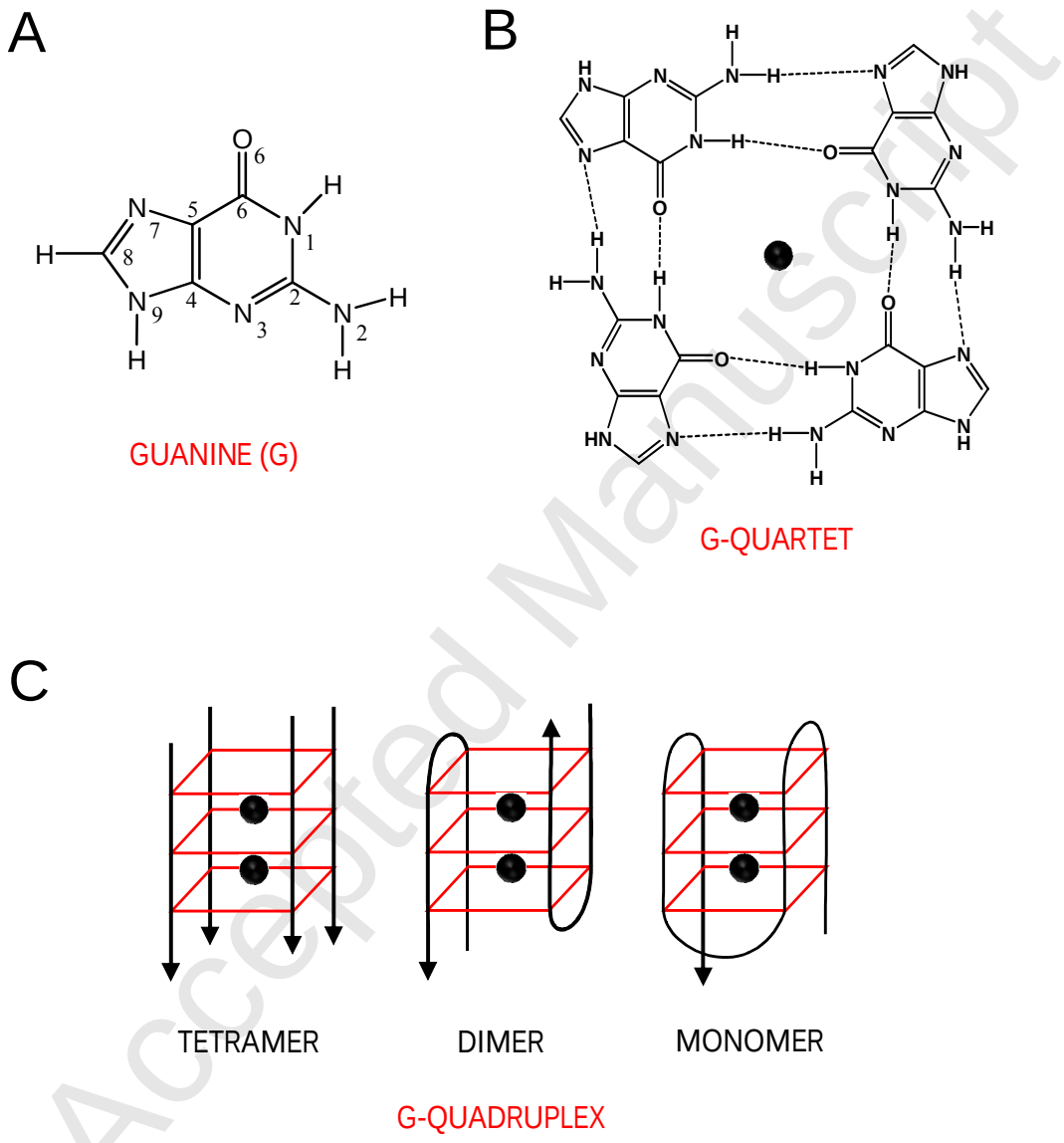

Scheme 1 (A) Chemical structure of guanine (G) base. (B) G-quartet (G_q) showing the hydrogen bonding between four planar G bases. (C) Schematic representation of tetramer, dimer and monomer G-quadruplexes composed by three staked G-quartets; the cations that stabilise the G-quadruplexes are shown as black balls.

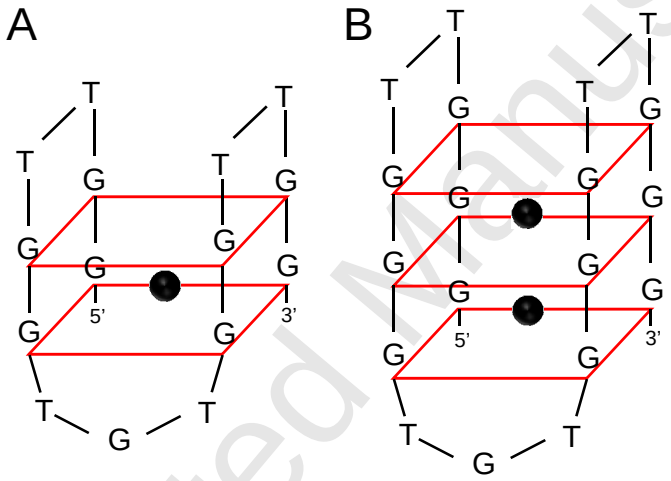

Scheme 2 Schematic representation of unimolecular antiparallel G-quadruplex structures formed by the thrombin binding aptamers: (A) 5'-GGTTGGTGTGGTTGG-3' (TBA) and (B) 5'-GGGTTGGGTGTGGGTTGGG-3' (eTBA).

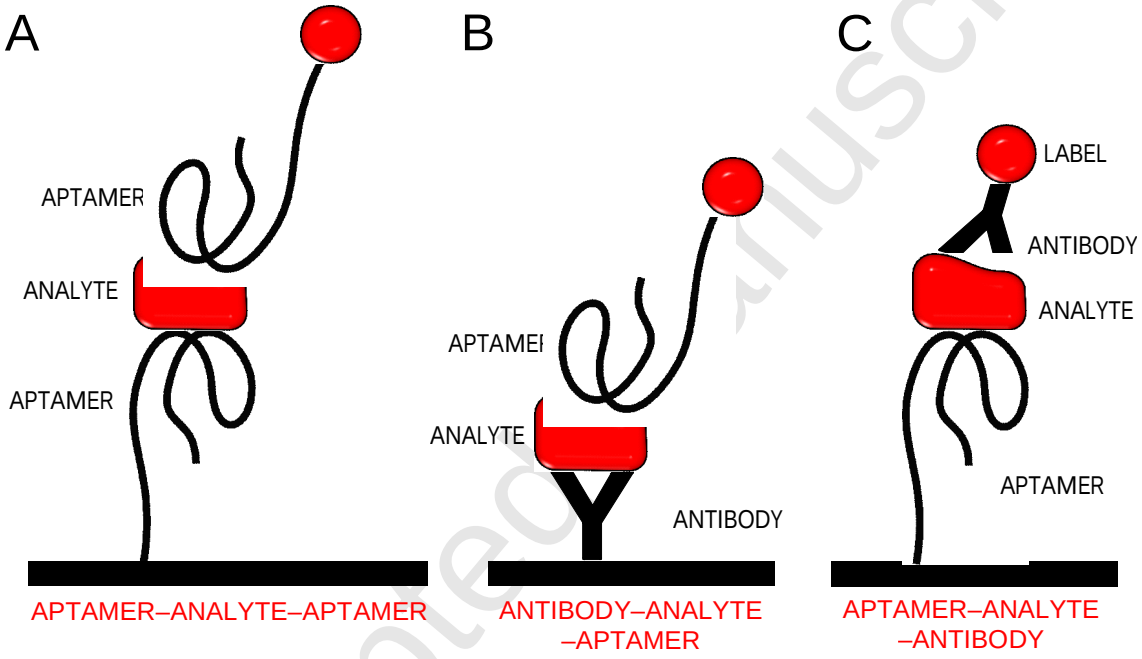

Scheme 3 Sandwich-type quadruplex aptasensors. (A) Aptamer–analyte–aptamer sandwich: the first aptamer is used for binding the analyte to the surface and the second labelled aptamer is used for detection. (B) Antibody–analyte–aptamer sandwich: the analyte is bound to the surface via an antibody and a labelled aptamer is used for detection; (C) Aptamer–analyte–antibody sandwich: the analyte is bound to the surface via an aptamer and a labelled antibody is used for detection.

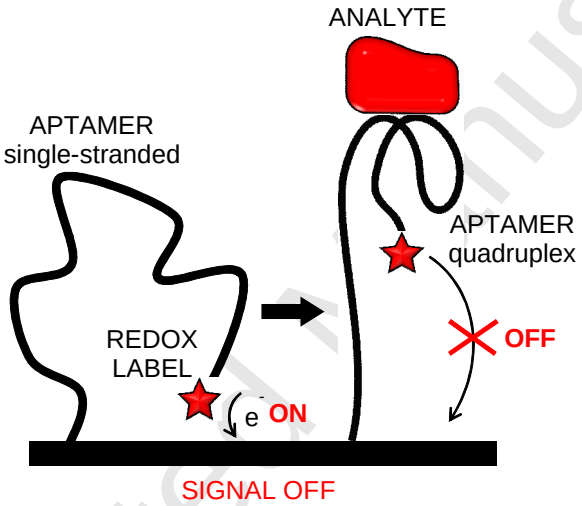

Scheme 4 Structure-switching quadruplex aptasensors; the analyte binding causes the aptamer conformational modifications and increases the distance from the redox label to the electrode.

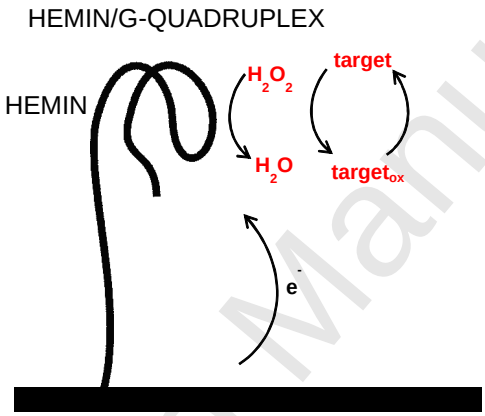

Scheme 5 Hemin/G-quadruplex peroxidase-mimicking DNAzymes electrochemical biosensor.

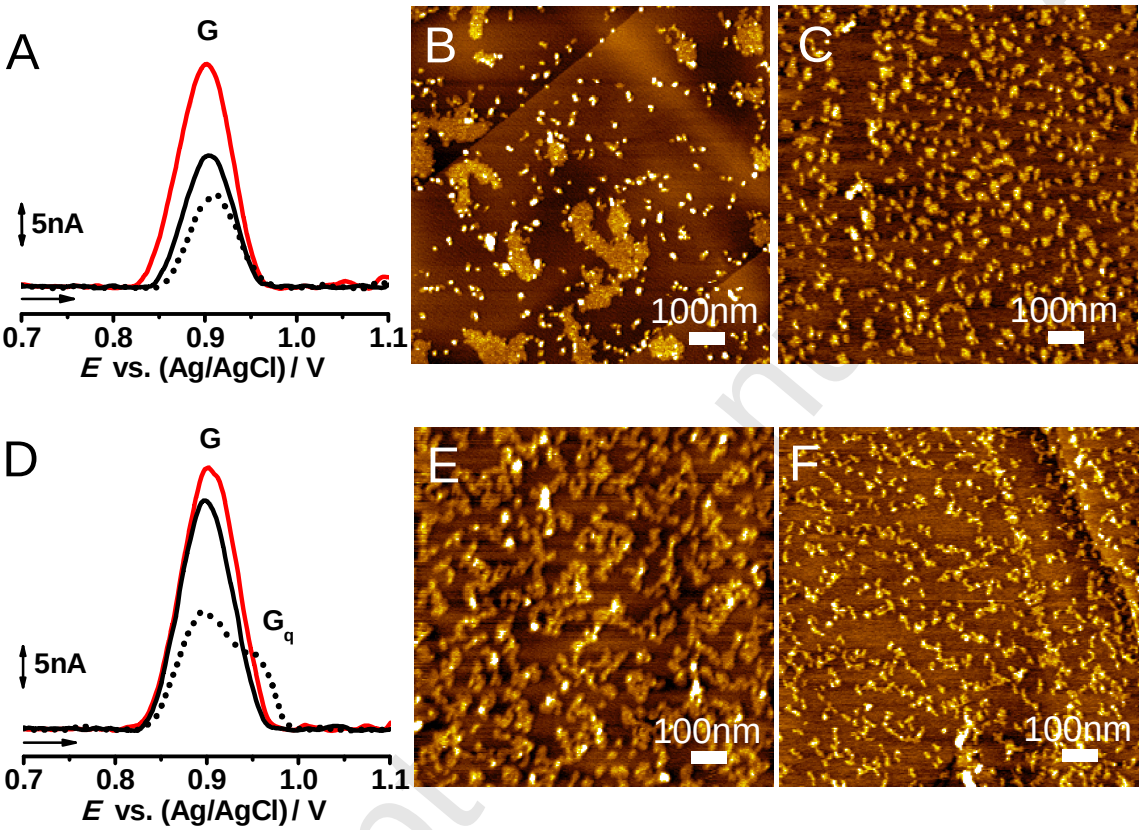

Fig. 1 (A, D) DP voltammograms baseline corrected, in 0.1 M NaH_2PO_4/Na_2HPO_4 buffer solution pH = 7.0, with 1 µg mL^{-1} (A) TBA and (D) eTBA, (—) in the absence and in the presence of 100 mM K^+, (—) 0 h and (•••) 24 h incubation. (B, C, E, F) AFM images of (B, C) TBA and (E, F) eTBA spontaneously adsorbed during 3 min, from solutions of 1 µg mL^{-1} TBA or eTBA in 0.1 M NaH_2PO_4/Na_2HPO_4 buffer solution pH = 7.0, (B, E) in the absence and (C, F) in the presence of 100 mM K^+, 24 h incubation. [Adapted from reference [28] with permission].

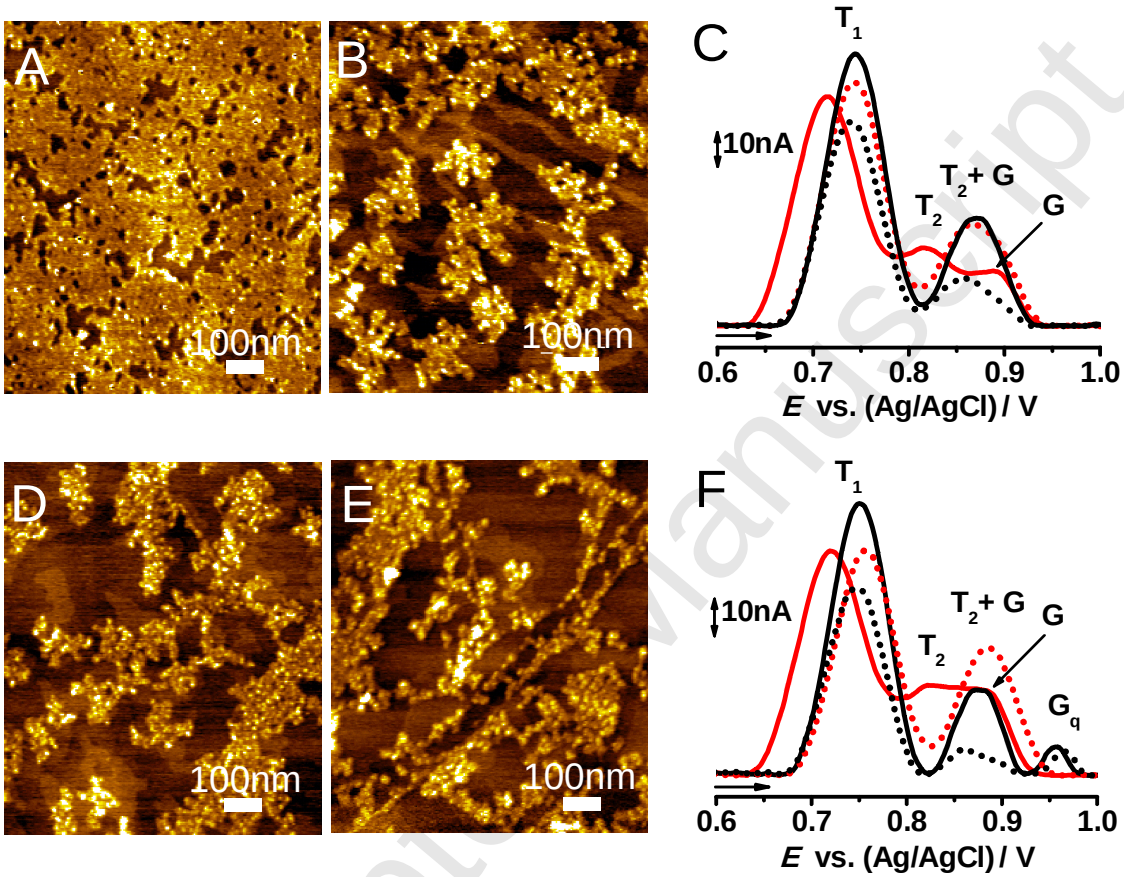

Fig. 2 (A, B, D, E) AFM images of complex (A, B) TBA–thrombin and (D, E) eTBA–thrombin, spontaneously adsorbed during 5 min from incubated solutions, in 0.1 M NaH_2PO_4/Na_2HPO_4 buffer solution pH = 7.0, of 1 μg mL^{-1} TBA or eTBA with 10 μg mL^{-1} thrombin, (A, D) in the absence and (B, E) in the presence of 100 mM K^+, 24 h of incubation. (C, F) DP voltammograms baseline corrected, in 0.1 M NaH_2PO_4/Na_2HPO_4 buffer solution pH = 7.0, with 1 μg mL^{-1} thrombin incubated with 1 μg mL^{-1} (C) TBA and (F) eTBA, in the absence of K^+, (▬) 0 h and (•••) 48 h incubation, and in the presence of 100 mM K^+, (▬) 0 h and (•••) 48 h incubation. [Adapted from reference [28] with permission].

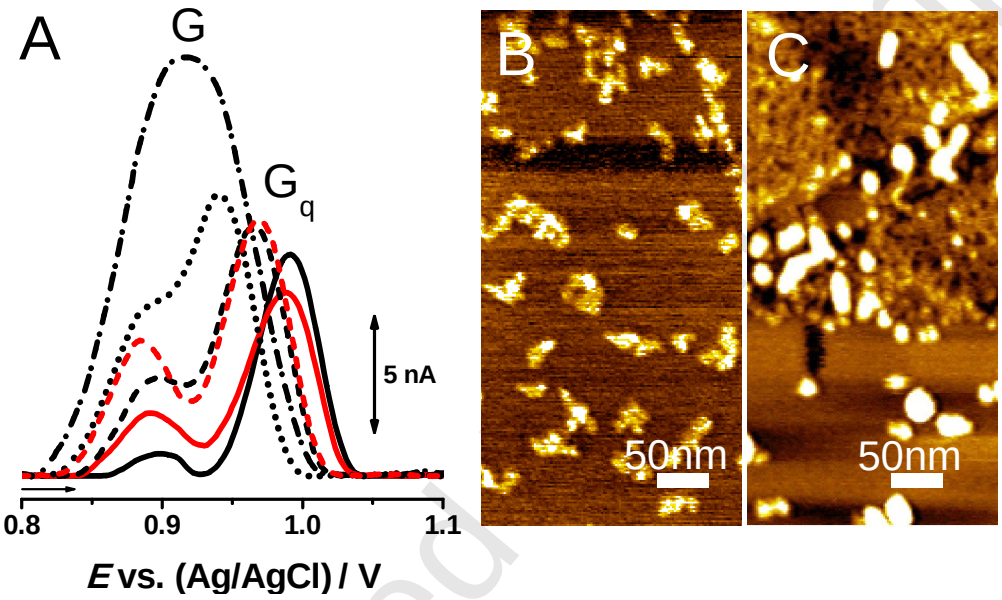

Fig. 3 (A) DP voltammograms baseline corrected in 3.0 µM $d(G)_{10}$, in 0.1 M NaH_2PO_4/Na_2HPO_4 buffer solution pH = 7.0, in the absence of K^+, (▪●▪) 0 h, (●●●) 24 h, (▪▪▪) 48 h and (—) 14 days incubation, and in the presence of 1 mM K^+ (▪▪▪) 0 h and (—) 24 h incubation. (B, C) AFM images of $d(G)_{10}$ spontaneous adsorbed from 0.3 µM $d(G)_{10}$, in 0.1 M NaH_2PO_4/Na_2HPO_4 buffer solution pH = 7.0, (B) 0 h and (C) 14 days incubation. [Adapted from reference [40] with permission].

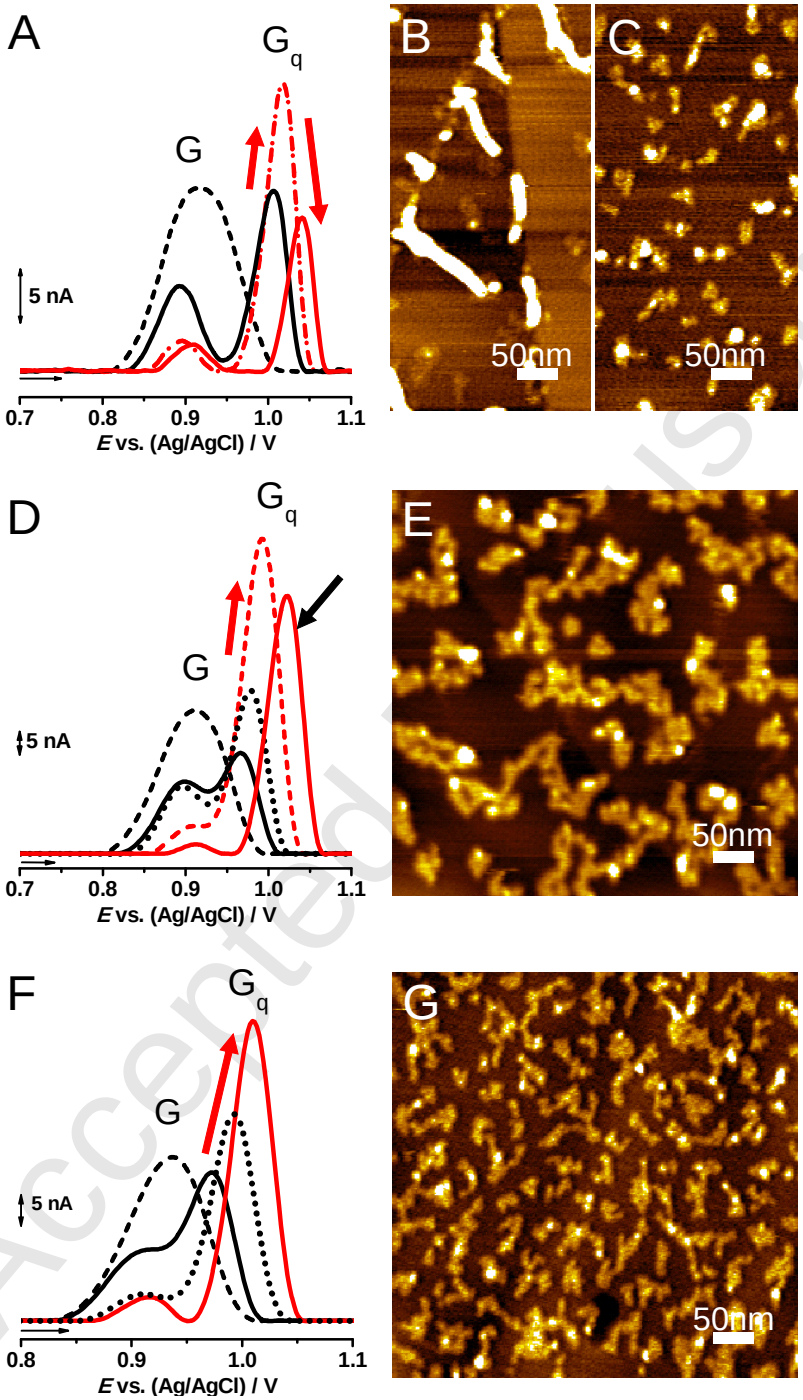

Fig. 4 (A, D, F) DP voltammograms baseline corrected, in 0.1 M NaH_2PO_4/Na_2HPO_4 buffer solution pH = 7.0, with 3.0 µM (A) $d(G)_{10}$, (D) $d(TG_9)$ and (F) $d(TG_8T)$, (▪▪▪) in the absence and in the presence of (—) 5 mM, (●●●) 50 mM, (▪●▪) 100 mM, (▪▪▪) 200 mM and (—) 1 M K^+, after 0 h incubation. (B, C, E, G) AFM images of (B, C) $d(G)_{10}$, (E) $d(TG_9)$ and (G) $d(TG_8T)$ spontaneous adsorbed from 0.3 µM $d(G)_{10}$, $d(TG_9)$ or $d(TG_8T)$, in 0.1 M

NaH_2PO_4/Na_2HPO_4 buffer solution pH = 7.0, in the presence of 200 mM K^+ ions, 24 h incubation. [Adapted from reference [40] with permission].